JPET Fast Forward. Published on July 23, 2008 as DOI: 10.1124/jpet.108.141143

JPET #141143

VIP increases CFTR levels in the apical membrane of Calu-3 cells through a PKC-dependent mechanism

Frédéric Chappe, Matthew E. Loewen, John W. Hanrahan and Valérie Chappe

Department of Physiology & Biophysics, Dalhousie University, Halifax, NS Canada (F.C., V.C.)

Department of Physiology, McGill University, Montréal, QC Canada (M. E. L., J. W. H.)

Running title: VIP increases apical CFTR channel density.

Corresponding author: Valérie Chappe, PhD. Department of Physiology & Biophysics, 5850 College Street, Halifax, NS Canada B3H 1X5. Phone: 902-494-2995 Fax: 902-494-1685; E-mail: valerie.chappe@dal.ca

Number of text pages: 30

Number of tables: 1

Number of figures: 9

Number of references: 39

Number of words in the Abstract: 238

Number of words in the Introduction: 431

Number of words in the Discussion: 1353

List of non-standard abbreviations:

BisX: bisindolylmaleimide X

ChCl: chelerythrine chloride

CFTR: Cystic Fibrosis Transmembrane conductance Regulator

RIPA: Radio-Immuno-Precipitation Assay

IBMX: 3-Isobutyl-1-methylxanthine

cpt-cAMP: 8-(4-Chlorophenylthio) adenosine-3′,5′-cyclic Monophosphosphate

$CFTR_{inh172}$ (3-[(3-Trifluoromethyl)phenyl]-5-[(4-carboxyphenyl)methylene]-2-thioxo-4-thiazolidinone)

H89: (N-[2-(p-Bromocinnamylamino)ethyl]-5-isoquinolinesulfonamide dihydrochloride)

Recommended section: Cellular and Molecular

Abstract

Non-cholinergic neurons contribute to innate airway defences by releasing VIP, which stimulates the submucosal glands to produce a bicarbonate rich fluid containing mucins and antimicrobial factors. VIP elevates cAMP and activates cystic fibrosis transmembrane conductance regulator (CFTR) channels; however its effects on surface expression have not been investigated. We studied CFTR levels in the apical membrane of polarized Calu-3 cell monolayers, a widely used model for submucosal gland serous cells. Biotinylation during VIP exposure revealed a significant increase in apical CFTR within 10 min, which reached a maximal 3.3-fold increase after 30 min. Total CFTR content of cell lysates was not altered during this time period, therefore the increase in surface CFTR reflects redistribution from intracellular pools. Internalization assays revealed that apical accumulation was due, at least in part, to a reduction in the rate of CFTR endocytosis. VIP-induced accumulation of apical CFTR was mimicked by phorbol ester but not by forskolin, and was blocked by the PKC inhibitors bisindolylmaleimide X (BisX) or chelerythrine chloride but not by the PKA inhibitor H89. Increases in surface expression were paralleled by enhanced iodide effluxes during cAMP stimulation. BisX inhibition of VIP responses was abrogated when monolayers were pre-treated with tannic acid to inhibit endosome recycling. Thus PKC increases the surface expression of CFTR channels in addition to potentiating their responsiveness to PKA phosphorylation. Integrated regulation through multiple signalling pathways may be a common feature of VIP and other physiological secretagogues.

Introduction

The Cystic Fibrosis Transmembrane conductance Regulator (CFTR) is a tightly regulated ion channel which mediates cAMP-stimulated anion conductance in epithelia and other cell types. It contains twelve membrane spanning regions (TM1-TM12) which may surround the channel pore, two nucleotide binding domains (NBD1, NBD2) which control ATP-dependent gating, and a highly charged regulatory (R) domain which mediates channel activation by protein kinase A and C phosphorylation (Riordan et al., 1989). Mutations in the CFTR gene that reduce its channel function or cause CFTR retention in the endoplasmic reticulum lead to cystic fibrosis (CF), the most common lethal genetic disease in Caucasian populations (Gadsby et al., 2006). CF is characterized by reduced chloride secretion across epithelia, viscous mucus secretions, chronic bacterial infections, and inflammation in the airways. Conversely, hyperstimulation of CFTR channels during bacterial infection of the intestine by *Vibrio cholerae* may result in secretory diarrhea, dehydration, acidosis and death (Thiagarajah and Verkman, 2003).

CFTR is activated by protein kinase A (PKA)-dependent phosphorylation. Exposing the cytosolic aspect of CFTR channels to PKC enhances their subsequent responsiveness to PKA activation (Jia et al., 1997; Tabcharani et al., 1991); in part through direct PKC phosphorylation of the R domain (Chappe et al., 2003; Chappe et al., 2004). Moreover, phorbol esters potentiate cAMP-stimulated chloride conductance in *Xenopus* oocytes heterologously expressing CFTR (Sullivan et al., 1991), and similar effects have been reported in the human colonic HT-29 cell line (Bajnath et al., 1993) and in isolated rat pancreatic duct cells (Winpenny et al., 1995). Although mutagenesis studies indicate that these responses depend, at least in part, on direct phosphorylation of CFTR (Chappe et al., 2003; Chappe et al., 2004), PKC could also act through other mechanisms. For example, studies of HT-29 cells suggest that PKC stimulation can

increase the number of functional CFTR channels in apical membrane patches (Bajnath et al., 1993).

To date, most studies of CFTR regulation by PKC have utilized purified kinases or artificial activators rather than physiological secretagogues. Vasoactive intestinal peptide (VIP) is the major physiological stimulus for CFTR-dependent secretion by serous cells of the airway sub-mucosal glands (Ianowski et al., 2007; Wine and Joo, 2004). Although VIP was initially considered as a cAMP-mediated secretagogue, it has recently been shown to regulate CFTR through both PKA- and PKC-dependent signaling pathways (Derand et al., 2004; Laburthe et al., 2007). Since VIP is a physiological agonist that may act on multiple signaling pathways, we examined whether it elevates the surface expression of CFTR channels at the apical membrane in polarized Calu-3 cell monolayers, a widely used model for serous cells in human airway submucosal glands.

Methods

Chemicals. Cell culture media and supplements were purchased from GIBCO (NY, USA); sulfo-NHS-SS-Biotin was from Pierce, (Madison, WI, USA); streptavidin coated beads were from Novagen/EMD Chemicals Inc.(La Jolla, CA, USA); M3A7 monoclonal anti-CFTR antibody was from Upstate (Charlottesville, VA, USA); goat anti-mouse secondary antibody conjugated to peroxidase was from Jackson ImmunoResearch Lab., Inc. (West Grove, PA, USA); ECL+ chemiluminescence detection kits were from GE Healthcare (Amersham**,** Bucks, UK); other chemicals were from Sigma (St. Louis, MO, USA) and of the highest grade available.

Cell culture. Cells were cultured in α–Minimum Essential Medium supplemented with 15% foetal bovine serum, 1% penicillin-streptomycin, 1% non-essential amino acids, and 1% sodium pyruvate with 5% CO_2 at 37^{o}C. For apical biotinylation experiments, Calu-3 cells were cultured in transwells (24 mm diameter with 0.4 μM diameter pores; Corning Life Sciences, Acton, MA, USA) at the air-liquid interface until they formed tight monolayers. For short-circuit current studies, Calu-3 cells were seeded on clear polyester Snapwells (1 cm^2 diameter, 0.4μm pores; Corning Life Science, Acton, MA, USA) at a density of 2 x 10^6 cells/per well. After 7 days, apical medium was removed and monolayers were maintained at the air-liquid interface for 14 days. The apical surface was washed with phosphate buffered saline and the basolateral medium was changed every 4 days.

Cell surface biotinylation. Calu-3 cells were cultured on porous supports at the air-liquid interface until they formed tight monolayers and no medium leakage to the apical side was observed. Biotinylation experiments were performed as described previously (Chappe et al., 2005). Biotinylated proteins were eluted from streptavidin beads using 5X sample buffer

containing dithiothreitol (DTT) to cleave the NHS-S-S-biotin and Western blotted with the monoclonal anti-CFTR antibody M3A7. *Experimental design:* VIP or (other drugs) was added directly into complete culture medium in the basolateral compartment for 5 min to 2 hrs (or as indicated on individual figures) at 37°C, and proteins in the apical membrane were labeled at 4°C with the cleavable and membrane impermeant sulfo-NHS-SS-biotin, then pulled down as before (Chappe et al., 2005). To assess the role of PKC or PKA in mediating the VIP-stimulated increase in apical CFTR expression, PKC or PKA activators/inhibitors were added in the apical compartment filled with complete culture medium for indicated periods (at 37°C) prior to biotinylation. Inhibitors were added 30 min before VIP. Apical CFTR was quantified by densitometry of scanned Western blots and results (in arbitrary units) were corrected for non-specific CFTR binding to the beads by subtraction of the background signal when biotin was omitted from the reaction mix. Corrected densities were then normalized to the corresponding controls.

CFTR internalization assays. Apical CFTR internalization was measured according to R. Ganeshan *et al* (2007). Briefly, cells were biotinylated on ice as described above, returned to 37°C for the indicated periods, placed on ice again and membranes were stripped of biotin by incubation with a membrane-impermeant stripping solution (mM): 100 MESNA (mercaptoethane-sulfonic acid), 50 Tris, 100 NaCl, 1 EDTA, 0.2 % BSA, pH 8.0, for 15 minutes (repeated three times). Cells were then harvested by scraping and lysed in RIPA buffer on ice for 30 min. Remaining (intracellular) biotinylated proteins were pulled down on streptavidin-coated beads and visualized on Western blots as described. *Experimental design:* Cells were incubated with VIP for 30 min (or not: control) prior to biotinylation at 4 ^{o}C, then returned to 37°C to enable the labeled protein to be internalized for 0, 5, 15 or 30 minutes, in the absence (control) or

presence of VIP for the indicated periods. After this timed incubation at 37°C, cells were placed on ice and any biotin remaining on the apical surface was cleaved by exposure to stripping solution. The amount of internalized CFTR present in streptavidin pull downs, after stripping biotin from the cell surface, was estimated by densitometry of scanned Western blots (probed with M3A7 anti-CFTR antibody) and densities were normalised to total apical CFTR biotinylated (no incubation at 37°C and no membrane stripping). The amount of labeled CFTR that was precipitated immediately after biotinylation at 4°C was taken as a measure of total surface CFTR (100%) when calculating the percentage of CFTR that had been internalized. The absence of CFTR in pull downs from cells where membranes had been stripped immediately after biotinylation at 0°C confirmed the efficiency of biotin cleavage by the stripping solution, and also the specificity of cell surface biotinylation.

Iodide effluxes. Cells were cultured in six-well plates for 3-7 days. Confluent monolayers were used, and iodide effluxes were assayed as described previously (Chappe et al., 2003). The iodide concentration of each aliquot was measured using an iodide sensitive electrode (Thermo Electron Corporation, MA, USA), and the I^- efflux rate constant k (min^{-1}) was calculated according to Becq *et al.*, (2003; European working group on CFTR expression). *Experimental design:* Activators or inhibitors were included in the efflux buffer from time 0, and collection continued at 1 min intervals for a further 12 min in the continued presence of tested compounds. The first three samples (time = -2 to 0 min) were used to establish a stable baseline of efflux. To test the effect of VIP exposure on halide permeability, control iodide efflux experiments were performed using Calu-3 cell monolayers that had been incubated with 300 nM VIP for 30 min to 2 hrs prior to the efflux experiment. We then measured basal iodide release

during the first minute after removing extra-cellular iodide loading buffer; or calculated efflux rate for the entire efflux experiment without any acute stimulation.

Immunoblotting. Membrane proteins were solubilized on ice for 30 min in RIPA buffer, 100μg of proteins were subjected to 7.5% SDS-PAGE, transferred to PVDF membranes and probed with M3A7 monoclonal anti-CFTR antibody as reported previously (Chappe et al., 2003). Densitometry of scanned Western blots, using ImageJ software (NIH, http://rsb.info.nih.gov/ij/), was used to estimate CFTR density in each condition. Only the complex glycosylated, band C form of CFTR can be readily detected in Calu-3 cells that are cultured on permeable supports (J. Liao, unpublished observation).

Short-circuit current measurements. Snapwells with differentiated Calu-3 cells monolayers were mounted in modified Ussing chambers (Easymount, Physiologic Instruments, San Diego, CA) and equilibrated for 20 min in standard Krebs bicarbonate-Ringer's solution containing 10mM glucose. The epithelium was voltage clamped at 0 mV and 10 mV pulses were used to monitor resistance before and after adding agonists. The short-circuit current (Isc) needed to clamp the transepithelial potential at 0 mV was recorded using a Powerlab (ADInstruments, Colorado Springs, CO) analogue-to-digital data acquisition system.

Statistics. Results are reported as the means ± S.E.M., n= number of independent experiments. Differences were assessed using the Student's t-test, with $p < 0.05$ considered significant. $*p < 0.05$, $**p < 0.01$, and $***p < 0.001$.

Results

VIP increases the amount of CFTR protein in the apical membrane of Calu-3 cells. CFTR conductance could increase due to activation of its gating (i.e. an increase in open probability, P_o) and/or to an increase in its surface expression (i.e. the number of channels in the membrane, N). To test the latter possibility we used biotinylation to quantify surface CFTR in polarized Calu-3 cells after adding 300 nM VIP to the basolateral side, where the VPAC1 receptor for VIP has been identified (Derand et al., 2004). As shown in Figure 1B, apical CFTR increased during VIP exposure to 169.8 % ± 22.2 after 10 min (n = 4, $p < 0.037$), reaching a peak of 334.4 % ± 79.3 (n = 7, $p < 0.0023$) above control levels after 30 min, and remained more than 2-fold above control levels during >2 hrs of continuous VIP exposure (227.0% ± 68.8, n = 6, $p < 0.01$).

Role of PKC in VIP-induced elevation of CFTR surface expression. Previous studies have suggested that PKC may influence apical CFTR trafficking in addition to increasing channel open probability (Bajnath et al., 1995; Barthelson et al., 1987). Pretreating cells with the PKC inhibitor bisindolylmaleimide X (BisX; 500 nM) for 30 min did not change the level of apical CFTR expression under control conditions (BisX alone: 118.2± 13.1% of control, $p > 0.55$) but abolished the VIP stimulated increase in surface CFTR; (VIP 20 min + BisX: 90.0 ± 27.1% of control, $p > 0.51$; VIP 30 min + BisX: 118.0 ±1 9.0 % of control, $p > 0.35$; Fig. 2A&D). VIP-stimulated increases in apical membrane CFTR were also strongly inhibited by pretreatment with 10 μM chelerythrine chloride (ChCl), another PKC inhibitor which is structurally distinct from BisX (VIP 30 min + ChlCl: 111.2 ± 11.6% of control, $p > 0.45$; Fig. 2B&E). To further investigate the role of PKC in the VIP response, we examined the effect of a phorbol ester (PMA)

on apical CFTR expression (Fig 3). Exposure to 20 nM PMA for 30 or 120 min caused striking increases in surface CFTR (185.1 ± 58.9% of control, n = 4, $p < 0.04$ and 190.4 ± 35.1% of control, n=4, $p < 0.0025$, respectively), and this stimulation was inhibited by pre-treating cells with the PKC inhibitor BisX (500nM). With prolonged (24 hrs) PMA treatment to downregulate PKC, the amount of apical membrane CFTR declined to control levels (96 ± 13.67%, n = 4, $p > 0.68$).

PKC, but not PKA, signaling increases apical CFTR surface expression. The contribution of increased channel density to cAMP-stimulated secretion appears to vary with cell type. Since VIP raises intracellular [cAMP] in secretory epithelia, which might affect apical CFTR density transiently, we carried out time course experiments with forskolin. In marked contrast to the results obtained with VIP or PMA, the amount of surface CFTR was not affected by 5-30 min forskolin stimulation (Fig. 4 A&C; n = 4, $p > 0.097$). Similarly, the VIP-dependent increase in apical CFTR protein was unaffected by the PKA inhibitor H89 (Fig. 4B&D).

VIP reduces CFTR endocytosis rate. Total CFTR content in the cell lysates as monitored by Western blotting was not altered under any of the conditions used in our experiments (Table 1 and Fig. 1, 3, 4). This suggests that the increase in apical CFTR occurs through redistribution of an existing pool, most likely by recruitment from the recycling endosome compartment. To investigate the effect of VIP on endocytosis we performed internalization assays using polarized Calu-3 cells monolayers. Figure 5 shows that 42.6% ± 5.7 of the apical CFTR protein was internalized in 5 min at 37°C, and about 40 % remained at the surface after 15 - 30 min of internalization. However, on cells pre-treated with 300 nM VIP for 30 min, the amount of biotinylated CFTR internalized was markedly reduced when compared to

untreated cells, with only 12.5 % ± 2.7 of apical CFTR internalized in 5 min. This slow rate of retrieval from the surface remained constant for 30 min.

Functional effects of acute and short-term VIP exposure. To examine the functional significance of the observed increase in apical CFTR protein, we compared control and stimulated iodide effluxes using cells that had been pretreated, or not, with VIP or PMA. Acute stimulation of CFTR with VIP (100nM) or 250 μM cpt-cAMP + 1mM IBMX produced a large, transient stimulation that was detectable after 3 min and maximal after 5 min (Fig. 6). VIP stimulation was abolished by pre-treating cell monolayers with the PKA inhibitor H89 (10μM) or with the PKC inhibitor BisX (500 nM) for 30 min. The control efflux rate was not affected by including either inhibitor in the iodide loading solution for 30 min before the efflux ($p > 0.2$). Pre-incubating the monolayers with BisX also caused a modest but significant inhibition of the acute response to cpt-cAMP + IBMX (Fig. 6D). Pre-treating cells with PMA alone for 1 h did not affect the control iodide efflux rate, and acute stimulation by PMA + VIP (added at time 0 of the efflux) was similar to the response to VIP alone (Fig. 7A&B) as expected. By contrast, pre-treatment with PMA significantly enhanced subsequent responses to cpt-cAMP + IBMX or to VIP. The peak efflux rate during VIP stimulation was 0.37 ± 0.04 min^{-1} after cells had been pre-treated with PMA for 1h, compared to 0.26 ± 0.06 min^{-1} without PMA (Fig. 7). Similarly, the maximum efflux rate (peak) during cAMP + IBMX stimulation was elevated ~2-fold to 0.81±0.06 min^{-1} by PMA pretreatment. Also, pre-incubation with VIP for 30 min or 1h significantly enhanced halide permeability, such that efflux rates during the first 5 min were higher than during acute activation of CFTR by VIP (compare Fig. 8 B&C with Fig.6A). After 2 h of pre-incubation with VIP, the efflux rate was still higher than un-treated controls, although there was some decline when compared with shorter treatments (not shown). On cells pretreated

JPET Fast Forward. Published on July 23, 2008 as DOI: 10.1124/jpet.108.141143
This article has not been copyedited and formatted. The final version may differ from this version.

with VIP for 30min, iodide released during the first minute (t = -2, see *Materials and Methods*) was~1.7 times higher compared to untreated controls (Fig. 8A). Moreover, the iodide efflux elicited by 250 μM cpt-cAMP + 1 mM IBMX became maximal within 1 min and remained elevated for 5 min (Fig. 8E) when cell monolayers were pre-incubated with VIP for 30 min. The effect of VIP pre-treatment was abolished by 10 μM of CFTR inhibitor $CFTR_{inh172}$, which confirms that the increase in halide permeability was mediated by CFTR channels.

Effects of inhibiting PKC activity and membrane recycling on short-circuit current responses to VIP. The functional consequences of inhibiting PKC, and the role of CFTR recycling in polarized epithelial cells, were explored by measuring short-circuit current responses to VIP. Calu-3 monolayers that had been cultured at the air-liquid interface were mounted in modified Ussing chambers and equilibrated for 20 min in standard Krebs bicarbonate-Ringer's solution with 10 mM glucose. Exposure to 500 nM BisX for 25 min reduced the subsequent short-circuit current response to VIP by about half when compared with control monolayers (Fig. 9A, mean ± s.e., $n = 18$, $p < 0.05$). Interestingly, BisX sensitivity was abolished if the apical surface was pretreated with 0.05 % tannic acid for 10 min prior to VIP stimulation to inhibit both endocytosis and exocytosis (Fig. 9B). Moreover, adding tannic acid alone caused a small reduction in short-circuit current that was not different in the presence or absence of BisX (Fig. 9C).

Discussion

VIP is released from intrinsic airway neurons and serves as a physiological stimulus of CFTR-mediated secretion in airway submucosal glands. Although originally thought to signal exclusively through [cAMP], we have confirmed that at least part of the VIP response in polarized Calu-3 cell monolayers is mediated by activation of PKC (Derand et al., 2004), and we have explored the mechanism of this PKC regulation. VIP and phorbol ester both increased the surface expression of CFTR by several-fold without increasing the total amount of CFTR present in cell lysates. Since CFTR is rapidly internalized by highly efficient, clathrin-mediated endocytosis (Bradbury et al., 1994; Prince et al., 1994), the rate of endocytosis must be a determinant of steady-state surface expression level.

The carboxyl-terminus of CFTR contains tyrosine and di-leucine endocytic motifs (see review by (Ameen and Apodaca, 2007). Binding to the AP-2 adaptor complex drives the clathrin dependent endocytosis of CFTR, and the amino terminus of CFTR also modulates its surface stability through interaction with filamins and the actin cytoskeleton (Thelin et al., 2007). Although the mechanism of CFTR endocytosis has been studied in some detail, its regulation by physiological agonists is much less well understood. Using internalization assays we found that VIP reduces the rate of CFTR endocytosis in Calu-3 cells, as shown previously in the intestinal T84 cell line (Bradbury et al., 1992), while control internalization rate was consistent with values reported for apical CFTR endocytosis in Calu-3 and other polarized epithelial cells (Loffing et al., 1998; Varga et al., 2004). However in contrast to T84 cells where the action of VIP (Ameen and Apodaca, 2007) was mediated by cAMP, we found that inhibition of PKA by H89 did not block the increase in surface CFTR induced by VIP nor did elevating cAMP with forskolin mimic the effect of VIP on surface CFTR expression. These negative results are consistent with previous studies of Calu-3 (Chen et al., 2001; Loffing et al., 1998) and airway epithelial cells more

generally (Bertrand and Frizzell, 2003), thus airway cells may differ from other cell types with respect to their regulation of CFTR surface expression by cAMP.

Although VIP control over CFTR surface expression did not require PKA phosphorylation, it was critically dependent on PKC since two different PKC inhibitors blocked the VIP-induced increase in surface expression, and PMA mimicked the effect of VIP. There is a precedent for PKC inhibition of CFTR endocytosis in non-epithelial cells (Lukacs et al., 1997), however, its effects have not been explored in airway epithelial cells and the site of PKC phosphorylation and mechanism by which endocytosis is inhibited remain to be determined. Also, it will be important to learn if nucleotides and other physiological agonists that stimulate phospholipase C (and hence PKC) up-regulate the surface expression of CFTR as reported here. Stimulation of CFTR exocytosis and inhibition of its endocytosis may be linked with mucus release in Calu-3 and some other cells that express both CFTR and mucins (Berger et al., 1999). Apical P2Y2 receptors in the SPOC1 cell line, a model for rat airway goblet cells, trigger exocytosis and mucus release by activating PKCδ (Abdullah et al., 2003).

Importantly, no evidence for cAMP-stimulated exocytosis was obtained in two previous studies of Calu-3 cells that employed very different methodologies (Chen et al., 2001; Loffing et al., 1998). The regulation of surface CFTR levels by PKC has not been studied previously in Calu-3 cells, and we report here the first evidence that stimulating PKC increases apical CFTR surface expression in these cells. There is electrophysiological evidence for a phorbol ester-induced increase in apical CFTR channel density in the human colon cell line HT29 (Bajnath et al., 1993). PMA stimulates exocytosis in primary cultures of rat pancreatic duct by approximately 2.7-fold, and this is blocked by bisindolylmaleimide I (500nM), although effects on chloride conductance and CFTR surface expression have not been examined (Koh et al., 2000). There is also a precedent for PKC inhibition of CFTR endocytosis in non-epithelial CHO cells (Lukacs et al.,

1997), although PKC did not affect CFTR internalization in T84 intestinal epithelial cells (Bradbury and Bridges, 1992). Its effects have not been explored in airway epithelial cells and the site of PKC phosphorylation and mechanism by which endocytosis is inhibited remain to be determined.

In addition to PKC, phorbol esters can activate a family of "non-protein kinase C" (PKC) phorbol ester/diacylglycerol receptors called chimaerins, protein kinase D, RasGRPs, diacylglycerol kinase γ and Munc13 (Kazanietz, 2002). Munc13-1 is particularly relevant since it, rather than PKC, mediates phorbol ester-stimulated exocytosis in hippocampal neurons (Rhee et al., 2002), and high concentrations of PMA have been proposed to activate Munc13-2 in airway epithelial cells (Abdullah et al., 2003). For this reason we examined the sensitivity of both VIP- and PMA-induced surface expression of CFTR to the bisindolylmaleimide BisX. The bisindolylmaleimide PKC inhibitor BisX does not affect PKA at concentrations normally used to inhibit PKC. BisX and the structurally unrelated PKC inhibitor chelerythrine gave similar results, strongly suggesting that PKC mediates the VIP-induced increase in CFTR surface expression.

At the functional level, BisX (500nM) abolished VIP-stimulated iodide efflux whereas chelerythrine (1μM) caused < 50% inhibition in a previous study (Derand et al., 2004) The stronger effect of BisX is not surprising however, since it directly inhibits conventional (α, β, γ) PKC isozymes by binding at the ATP site (K_i = 16-20 nM) whereas chelerythrine disrupts substrate targeting through competition with the phosphoacceptor. Moreover chelerythrine has ~10-fold lower potency (K_i = 660 nM) compared to bisindolylmaleimide and causes little inhibition *in vitro* (Davies et al., 2000) presumably because it mainly affects targeting. Pre-incubating Calu-3 cell monolayers with BisX caused a modest but significant inhibition of the acute response to cpt-cAMP + IBMX. This is consistent with the role of PKC in potentiating

CFTR channel activation by PKA in CHO and BHK cells, where inhibition of cAMP responses by Gö6976 and chelerythrine have been reported previously (Chappe et al., 2003; Jia et al., 1997). Since VIP stimulation of iodide efflux was abolished by pre-treating cell monolayers with PKA or PKC inhibitors, our results support the hypothesis that CFTR activation by VIP is mediated by both PKA and PKC pathways in Calu-3 cells. PKC phosphorylation is known to weakly stimulate CFTR channel activity and dramatically enhance its response to PKA stimulation (Chappe et al., 2003; Jia et al., 1997; Tabcharani et al., 1991). To examine the functional significance of CFTR accumulation at the apical membrane, we also activated PKC directly using PMA and compared the response to that obtained by maximal concentrations of VIP (Derand et al., 2004) or cAMP + IBMX. PMA pre-treatment significantly enhanced subsequent responses to VIP or cpt-cAMP + IBMX, and VIP pre-incubation significantly enhanced halide permeability. This elevated activity after stimulation with high VIP concentrations or PKC would be consistent with an increase in the number of active CFTR channels at the plasma membrane. Short-circuit current responses in the presence of tannic acid (to inhibit recycling) are consistent with the biotinylation and iodide efflux data, but do not exclude the possibility that PKC enhances apical CFTR insertion, in addition to inhibiting its retrieval from the cell surface. Taken together these results strongly suggest that direct activation of CFTR gating by phosphorylation, and channel accumulation at the apical membrane have additive effects on macroscopic halide permeability.

In summary, we report here that a physiological agonist, VIP, increases the number of active CFTR channels in the apical membrane of the airway epithelial cell line Calu-3. This response is independent of PKA and is mediated by PKC since it is blocked by two structurally unrelated PKC inhibitors and mimicked by PMA exposure. The increase in surface expression is due, at least in part, to inhibition of constitutive endocytosis. Thus, VIP can act through converging

pathways to increase the secretory response. Such regulation by coordinated signaling may also occur *in vivo* during stimulation by multiple peptide hormones and transmitters that activate distinct signaling pathways, as reported for VIP and carbachol synergistic effect on mucus secretion (Choi et al., 2007). This emphasizes the importance of studying physiological secretagogues in addition to selective activators of particular signaling pathways.

References

Abdullah LH, Bundy JT, Ehre C, Davis CW. (2003) Mucin secretion and PKC isoforms in SPOC1 goblet cells: Differential activation by purinergic agonist and PMA. *Am J Physiol Lung Cell Mol Physiol* **285**:L149-L160.

Ameen N and Apodaca G. (2007) Defective CFTR apical endocytosis and enterocyte brush border in myosin VI-deficient mice. *Traffic* **8(8)**:998-1006.

Bajnath RB, Dekker K, De Jonge HR, Groot JA. (1995) Chloride secretion induced by phorbol dibutyrate and forskolin in the human colonic carcinoma cell line HT-29Cl.19A is regulated by different mechanisms. *Pflugers Arch* **430**:705-712.

Bajnath RB, Groot JA, De Jonge HR, Kansen M, Bijman J. (1993) Synergistic activation of non-rectifying small-conductance chloride channels by forskolin and phorbol esters in cell-attached patches of the human colon carcinoma cell line HT-29cl.19A. *Pflugers Arch* **425**:100-108.

Barthelson RA, Jacoby DB, Widdicombe JH. (1987) Regulation of chloride secretion in dog tracheal epithelium by protein kinase C. *Am J Physiol Cell Physiol* **253**:C802-C808.

Becq F., Auzanneau C. , Norez C., Dérand R. , and Bulteau-Pignoux L. (2003) Radiotracer flux method to study CFTR channel activity: regulation, pharmacology and drug discovery. *European Working Group on CFTR Expression* **D.5.** EFFLUX ASSAYS:1-13.

Berger JT, Voynow JA, Peters KW, Rose MC. (1999) Respiratory carcinoma cell lines. MUC genes and glycoconjugates. *Am J Respir Cell Mol Biol* **20**:500-510.

Bertrand CA and Frizzell RA. (2003) The role of regulated CFTR trafficking in epithelial secretion. *Am J Physiol Cell Physiol* **285**:C1-C18.

Bradbury NA and Bridges RJ. (1992) Endocytosis is regulated by protein kinase A, but not protein kinase C in a secretory epithelial cell line. *Biochem Biophys Res Commun* **184**:1173-1180.

Bradbury NA, Cohn JA, Venglarik CJ, Bridges RJ. (1994) Biochemical and biophysical identification of cystic fibrosis transmembrane conductance regulator chloride channels as components of endocytic clathrin-coated vesicles. *J Biol Chem* **269**:8296-8302.

Bradbury NA, Jilling T, Kirk KL, Bridges RJ. (1992) Regulated endocytosis in a chloride secretory epithelial cell line. *Am J Physiol Cell Physiol* **262**:C752-C759.

Chappe F, Loewen ME, Hanrahan, John W and Chappe,Valerie. (2006) VIP increases insertion of active CFTR channels in the apical membrane of Calu-3 cells by stimulating PKC signaling pathway. *Pediatr Pulmonol* **41(S29)**:210-210.

Chappe V, Hinkson DA, Howell LD, Evagelidis A, Liao J, Chang XB, Riordan JR, Hanrahan JW. (2004) Stimulatory and inhibitory protein kinase C consensus sequences regulate the cystic fibrosis transmembrane conductance regulator. *Proc Natl Acad Sci U S A* **101**:390-395.

Chappe V, Hinkson DA, Zhu T, Chang XB, Riordan JR, Hanrahan JW. (2003) Phosphorylation of protein kinase C sites in NBD1 and the R domain control CFTR channel activation by PKA. *J Physiol* **548**:39-52.

Chappe V, Irvine T, Liao J, Evagelidis A, Hanrahan JW. (2005) Phosphorylation of CFTR by PKA promotes binding of the regulatory domain. *EMBO J* **24**:2730-2740.

Chen P, Hwang TC, Gillis KD. (2001) The relationship between cAMP, ca(2)+, and transport of CFTR to the plasma membrane. *J Gen Physiol* **118**:135-144.

Choi JY, Joo NS, Krouse ME, Wu JV, Robbins RC, Ianowski JP, Hanrahan JW, Wine JJ. (2007) Synergistic airway gland mucus secretion in response to vasoactive intestinal peptide and carbachol is lost in cystic fibrosis. J Clin Invest. **117(10)**: 3118-3127.

Davies SP, Reddy H, Caivano M, Cohen P. (2000) Specificity and mechanism of action of some commonly used protein kinase inhibitors. *Biochem J* **351**:95-105.

Derand R, Montoni A, Bulteau-Pignoux L, Janet T, Moreau B, Muller JM, Becq F. (2004) Activation of VPAC1 receptors by VIP and PACAP-27 in human bronchial epithelial cells induces CFTR-dependent chloride secretion. *Br J Pharmacol* **141**:698-708.

Gadsby DC, Vergani P, Csanady L. (2006) The ABC protein turned chloride channel whose failure causes cystic fibrosis. *Nature* **440**:477-483.

Ganeshan R, Nowotarski K, Di A, Nelson DJ, Kirk KL. (2007) CFTR surface expression and chloride currents are decreased by inhibitors of N-WASP and actin polymerization. *Biochim Biophys Acta* **1773**: 192-200.

Ianowski JP, Choi JY, Wine JJ, Hanrahan JW. (2007) Mucus secretion by single tracheal submucosal glands from normal and cystic fibrosis transmembrane conductance regulator knockout mice. *J Physiol* **580**:301-314.

Jia Y, Mathews CJ, Hanrahan JW. (1997) Phosphorylation by protein kinase C is required for acute activation of cystic fibrosis transmembrane conductance regulator by protein kinase A. *J Biol Chem* **272**:4978-4984.

Kazanietz MG. (2002) Novel "nonkinase" phorbol ester receptors: The C1 domain connection. *Mol Pharmacol* **61**:759-767.

Koh DS, Moody MW, Nguyen TD, Hille B. (2000) Regulation of exocytosis by protein kinases and ca(2+) in pancreatic duct epithelial cells. *J Gen Physiol* **116**:507-520.

Laburthe M, Couvineau A, Tan V. (2007) Class II G protein-coupled receptors for VIP and PACAP: Structure, models of activation and pharmacology. *Peptides* **28**:1631-1639.

Loffing J, Moyer BD, McCoy D, Stanton BA. (1998) Exocytosis is not involved in activation of cl- secretion via CFTR in calu-3 airway epithelial cells. *Am J Physiol Cell Physiol* **275**:C913-C920.

Lukacs GL, Segal G, Kartner N, Grinstein S, Zhang F. (1997) Constitutive internalization of cystic fibrosis transmembrane conductance regulator occurs via clathrin-dependent endocytosis and is regulated by protein phosphorylation. *Biochem J* **328 (Pt 2)**:353-361.

Prince LS, Tousson A, Marchase RB. (1993) Cell surface labeling of CFTR in T84 cells. *Am J Physiol Cell Physiol* **264**:C491-C498.

Prince LS, Workman RB,Jr, Marchase RB. (1994) Rapid endocytosis of the cystic fibrosis transmembrane conductance regulator chloride channel. *Proc Natl Acad Sci U S A* **91**:5192-5196.

Rhee JS, Betz A, Pyott S, Reim K, Varoqueaux F, Augustin I, Hesse D, Sudhof TC, Takahashi M, Rosenmund C, Brose N. (2002) Beta phorbol ester- and diacylglycerol-induced augmentation of transmitter release is mediated by Munc13s and not by PKCs. *Cell* **108**:121-133.

Riordan JR, Rommens JM, Kerem B, Alon N, Rozmahel R, Grzelczak Z, Zielenski J, Lok S, Plavsic N, Chou JL. (1989) Identification of the cystic fibrosis gene: Cloning and characterization of complementary DNA. *Science* **245**:1066-1073.

Sullivan SK, Swamy K, Field M. (1991) cAMP-activated C1 conductance is expressed in xenopus oocytes by injection of shark rectal gland mRNA. *Am J Physiol Cell Physiol* **260**:C664-C669.

Tabcharani JA, Chang XB, Riordan JR, Hanrahan JW. (1991) Phosphorylation-regulated Cl- channel in CHO cells stably expressing the cystic fibrosis gene. *Nature* **352**:628-631.

Thelin WR, Chen Y, Gentzsch M, Kreda SM, Sallee JL, Scarlett CO, Borchers CH, Jacobson K, Stutts MJ, Milgram SL. (2007) Direct interaction with filamins modulates the stability and plasma membrane expression of CFTR. *J Clin Invest* **117**:364-374.

Thiagarajah JR and Verkman AS. (2003) CFTR pharmacology and its role in intestinal fluid secretion. *Curr Opin Pharmacol* **3**:594-599.

Varga K, Jurkuvenaite A, Wakefield J, Hong JS, Guimbellot JS, Venglarik CJ, Niraj A, Mazur M, Sorscher EJ, Collawn JF, Bebok Z. (2004) Efficient intracellular processing of the endogenous cystic fibrosis transmembrane conductance regulator in epithelial cell lines. *J Biol Chem* **279**:22578-22584.

Wine JJ and Joo NS. (2004) Submucosal glands and airway defense. *Proc Am Thorac Soc* **1**:47-53.

Winpenny JP, McAlroy HL, Gray MA, Argent BE. (1995) Protein kinase C regulates the magnitude and stability of CFTR currents in pancreatic duct cells. *Am J Physiol Cell Physiol* **268**:C823-C828.

Footnotes

This work was supported by grants from the Canadian Institutes of Health Research / Nova Scotia Health Research Foundation (CIHR/NSHRF) Regional Partnership and Dalhousie Medical Research Foundation (DMRF) to VC, and by grants from the Canadian Cystic Fibrosis Foundation (CCFF) to JWH and VC. VC is a CIHR scholar.

Present address for M. Loewen: Department of Anaesthesiology, Pharmacology and Therapeutics, University of British Columbia, Vancouver, BC Canada.

A preliminary report of this work has been presented (Chappe et al., 2006).

Legends for Figures

Figure 1. Basolateral application of 300 nM VIP increases the amount of CFTR at the apical membrane of Calu-3 cells. **A**, Representative Western blot of pull-downs showing the accumulation of biotinylated apical CFTR during VIP exposure for 5 to 120 min, compared to control level of apical CFTR (time 0). Lower panel: total CFTR in 100μg of protein from corresponding cell lysates. **B**, Changes in CFTR density expressed as a percentage of CFTR measured under control conditions. Values are means ± S.E.M for n= 4 independent experiments. Student's t-test was used to evaluate significant difference vs control; ns (not significant): $p > 0.05$; ** $p < 0.01$.

Figure 2. PKC inhibitors abolish the VIP-induced increase in apical CFTR. Polarised Calu-3 cells were treated with 500 nM BisX or 10 μM Chelerythrine chloride (ChCl) for 30 min before adding 300 nM VIP to the basolateral compartment for 5 - 30 min. Representative Western blots of biotinylated apical CFTR are shown in **A** and **B**. **C**, Representative Western blot showing total CFTR present in 100 μg of lysate from control cells (1), and cells treated for 30 min with 300 nM VIP (2), 300 nM VIP + 500nM BisX (3), or 300 nM VIP + 10 μM Chelerythrine (4). **D & E**, Changes in apical CFTR levels estimated by densitometry of scanned Western blots and normalised to the control level of apical CFTR. Values are the means ± S.E.M for n=4-6 independent experiments. Student's t-test was used to evaluate significant differences vs control, vs VIP + Bis X, or VIP + ChCl; ns (not significant): $p > 0.05$; ** $p < 0.01$.

Figure 3. PMA stimulation increases the amount of CFTR at the apical membrane. **A**, Representative Western blot of apical CFTR (upper panel) under control condition or after stimulation by PMA for 2hrs, or PMA + BisX (500nM). Total CFTR present in cell lysates is shown in the lower panel. **B**, Representative Western blot showing biotinylated apical CFTR (upper panel) and total CFTR present in cell lysates (lower panel) from control, polarized monolayers (time 0), or monolayers stimulated for 2 h or 24 h with 20 nM PMA. **C**, Apical and total CFTR density. **D**, Western blot showing total CFTR present in 100 μg of lysate protein from untreated cells (1), or cells treated with PMA for 30 min (2), 1 h (3), 2 h (4) or 24 h (5). Values are the means ± S.E.M, for n=4 independent experiments. Student's t-test was used to evaluate significant difference vs control; ns (not significant): $p>0.05$; *$p < 0.05$; ** $p < 0.01$.

Figure 4. Modulating PKA activity did not affect apical membrane expression of CFTR. **A**, Representative Western blot of apical CFTR in pull downs from cells treated with 20 μM forskolin (FSK) for the indicated periods. Total CFTR present in 100 μg of lysate protein is shown in the lower panel. ***B***, Representative Western blot showing apical CFTR biotinylated after 30 min stimulation with 300 nM VIP, or 30 min pre-treatment with10 μM H89 followed by 300 nM VIP for an additional 30 min. Total CFTR present in 100 μg of lysate protein is shown in the lower panel. **C&D**, Changes in CFTR densities. Values are the means ± S.E.M, for n=4 independent experiments. Student's t-test was used to evaluate significant difference vs control; ns (not significant): $p > 0.05$.

Figure 5. VIP slows the rate at which apical CFTR is internalized. Endocytosis was quantified by measuring the retrieval of biotinylated CFTR into polarized Calu-3 cell monolayers. **A**,

Representative Western blot showing total surface CFTR immediately after biotinylation (control or VIP) and internalized CFTR after 0, 5, 15, and 30 min in control monolayers (upper panel) or monolayers pre-treated with VIP (300 nM) for 30 min before biotinylation (lower panel). **B,** The percent of CFTR remaining on the cell surface after incubation at 37°C are plotted vs incubation time for monolayers pre-treated (dark squares) or not (open triangles) with 300 nM VIP. Values are mean ± S.E.M, for n = 5 independent experiments. Student's t-test was used to evaluate significant difference vs control; ns (not significant): $p > 0.05$; $^{**}p < 0.01$; $^{***}p < 0.001$.

Figure 6. Role of protein kinases A and C during acute stimulation of CFTR channel activity by VIP and cAMP. **A**, Iodide efflux from Calu-3 cells under control conditions (squares) and after addition of 100 nM VIP (triangles) at time 0. **B**, Iodide efflux responses to 100 nM VIP (added at time 0) on untreated cells (triangles) or after pre-treatment with 10 μM H89 for 30min (circles). **C**, Effect of pre-treating cells with 500 nM BisX for 30 min on control (circles) or VIP-stimulated iodide efflux (triangles). For comparison, control efflux without pre-treatment is shown (squares). **D**, Iodide efflux responses to 250 μM cpt-cAMP + 1 mM IBMX (added at time 0) on untreated cells (triangles) or after pre-treatment with 500 nM BisX for 30 min (circles). Values are the means ± S.E.M, for n=3-6 independent experiments, each performed in duplicate. Student's t-test was used to evaluate significant difference vs control or vs cpt-cAMP + IBMX (**D**); ns (not significant): $p > 0.05$; $^{*}p < 0.05$; $^{***}p < 0.001$.

Figure 7. Effect of PMA pre-treatment on CFTR activation by VIP or cAMP. **A**, I^- efflux was measured under control conditions on cell monolayers pre-treated (diamond) or not (squares) with 20 nM PMA for 1h. **B,** Iodide efflux responses to 20n M PMA + 100 nM VIP added at time

0 (open circles) or 100 nM VIP alone (triangles) on control cells compared to the stimulation by 100 nM VIP of cell monolayers pre-treated with PMA for 1 h (filled circles). **C**, Iodide efflux responses to stimulation at time 0 with 250 μM cpt-cAMP + 1 mM IBMX of control cells (triangles) or PMA pre-treated cells (circles). Values are means ± S.E.M, for n=3-4 independent experiments performed in duplicate. Student's t-test was used to evaluate significant difference vs PMA pre-treated cells: ns = $p > 0.05$; **$p < 0.01$; ***$p < 0.001$.

Figure 8. Increased halide permeability of cell monolayers after pre-treatment with VIP. **A**, Spontaneous iodide release, during the first minute of efflux, by cell monolayers pre-treated with VIP for 30 min – 2 h. **B&C**, Control efflux rates calculated from untreated cell monolayers (squares) or cell monolayers pre-treated with 300 nM VIP (triangles) for 30 min (**B**) or 1h (**C**). **D**, Control efflux rates calculated from cell monolayers pre-treated with 300nM VIP for 1h in presence (open circles) or absence (triangles) of 10 μM CFTR inhibitor $CFTR_{inh172}$. **E**, Iodide efflux responses to 250 μM cpt-cAMP + 1mM IBMX (added at time 0) on cell monolayers pre-treated (circles) or not (triangles) with 300 nM VIP for 30 min. Values are means ± S.E.M, for n=3 independent experiments performed in duplicate. Student's t-test was used to evaluate significant difference vs control (**A-C**), vs $CFTR_{inh172}$ (**D**) or vs cAMP + IBMX on untreated cells (**E**). *$p < 0.05$, **$p < 0.01$; ***$p < 0.001$.

Figure 9. Role of PKC during VIP stimulation of short-circuit current across polarized Calu-3 monolayers. **A**, Effect of 500 nM BisX on the short-circuit current induced by 100 nM VIP. Control n = 18 and BisX n = 18, means ± S.E.M., (*) difference significant at $p < 0.05$. *B*, Inhibiting vesicle trafficking with 0.05% tannic acid (pH = 7.4 in Krebs bicarbonate-Ringer) eliminated the inhibition of VIP-induced short-circuit current by 500 nM BisX. **C**, Tannic acid

alone caused a small decrease in short-circuit current when added to unstimulated monolayers. Control n = 13 and BisX n = 13, ± SEM, difference not significant. **D**, Representative short-circuit current traces of VIP-stimulated short-circuit current and the effect of pre-treatment with 500 nM BisX. **E**, Representative traces showing that the VIP-induced short-circuit was not BisX sensitive after exposure to tannic acid, consistent with the proposed role of PKC in CFTR endocytosis.

JPET Fast Forward. Published on July 23, 2008 as DOI: 10.1124/jpet.108.141143
This article has not been copyedited and formatted. The final version may differ from this version.

Table 1. Total CFTR protein in cell lysates after indicated treatments. CFTR density measured under each condition is expressed as the percent of CFTR in control (untreated) cells. Values are mean ± S.E.M, for n= 4-6 independent experiments. Student's t-test was used to evaluate significance of differences vs control, with $p > 0.05$ considered not significantly different from control.

Treatment	Mean (% of control)	± S.E.M	*p* value
no biotin	100.75	12.91	0.91
VIP 30min	108.84	6.65	0.10
VIP 2hrs	103.86	7.25	0.49
BisX	100.29	1.99	0.95
ChlCl	104.25	11.63	0.64
H89	97.28	9.69	0.68
VIP+BisX	96.27	3.42	0.47
VIP+ChlCl	97.19	8.57	0.57
VIP+H89	100.72	3.93	0.78
PMA 30min	104.23	8.79	0.45
PMA 2hrs	110.74	11.14	0.11
PMA 24hrs	96.85	3.16	0.50
FSK 30min	96.38	3.64	0.21

Figure 1

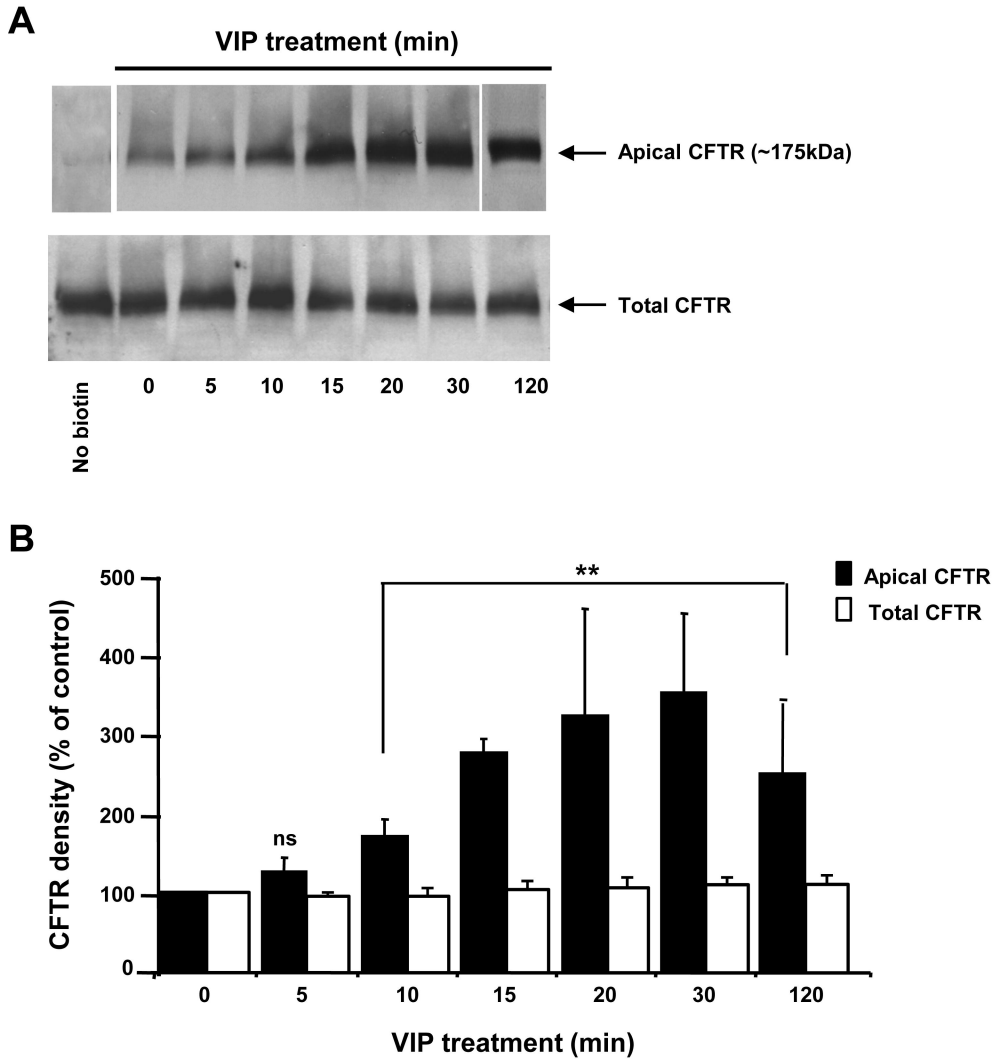
A
VIP treatment (min)
Apical CFTR (~175kDa)
Total CFTR
No biotin
0
5
10
15
20
30
120
B
**
Apical CFTR
Total CFTR
CFTR density (% of control)
500
400
300
200
100
0
ns
0
5
10
15
20
30
120
VIP treatment (min)

Figure 2

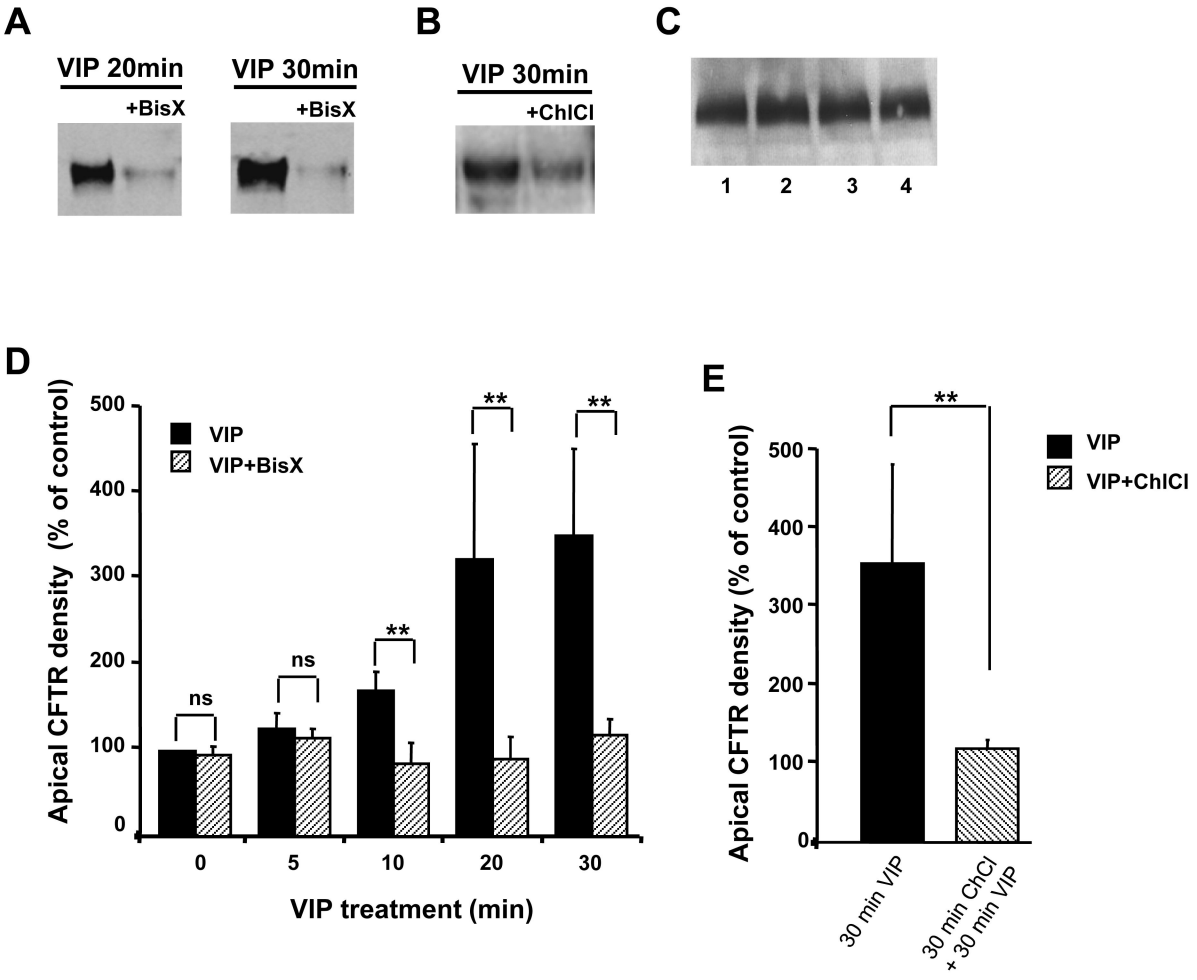
A
VIP 20min
+BisX
VIP 30min
+BisX
B
VIP 30min
+ChICl
C
1
2
3
4
D
Apical CFTR density (% of control)
500
400
300
200
100
0
VIP
VIP+BisX
ns
ns
**
**
**
0
5
10
20
30
VIP treatment (min)
E
Apical CFTR density (% of control)
500
400
300
200
100
0
**
VIP
VIP+ChICl
30 min VIP
30 min ChCl
+ 30 min VIP

Figure 3

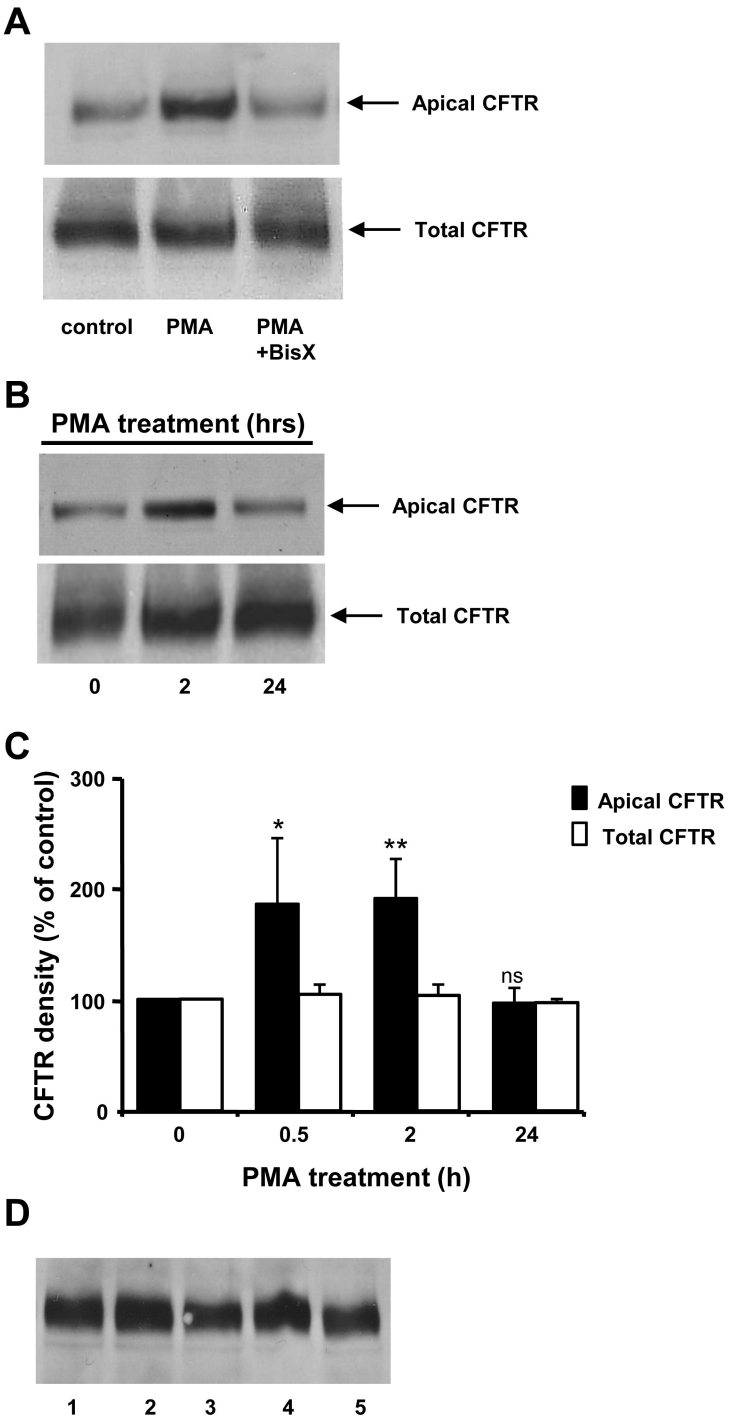
A
Apical CFTR
Total CFTR
control
PMA
PMA +BisX
B
PMA treatment (hrs)
Apical CFTR
Total CFTR
0
2
24
C
CFTR density (% of control)
300
200
100
0
*
**
ns
Apical CFTR
Total CFTR
0
0.5
2
24
PMA treatment (h)
D
1
2
3
4
5

Figure 4

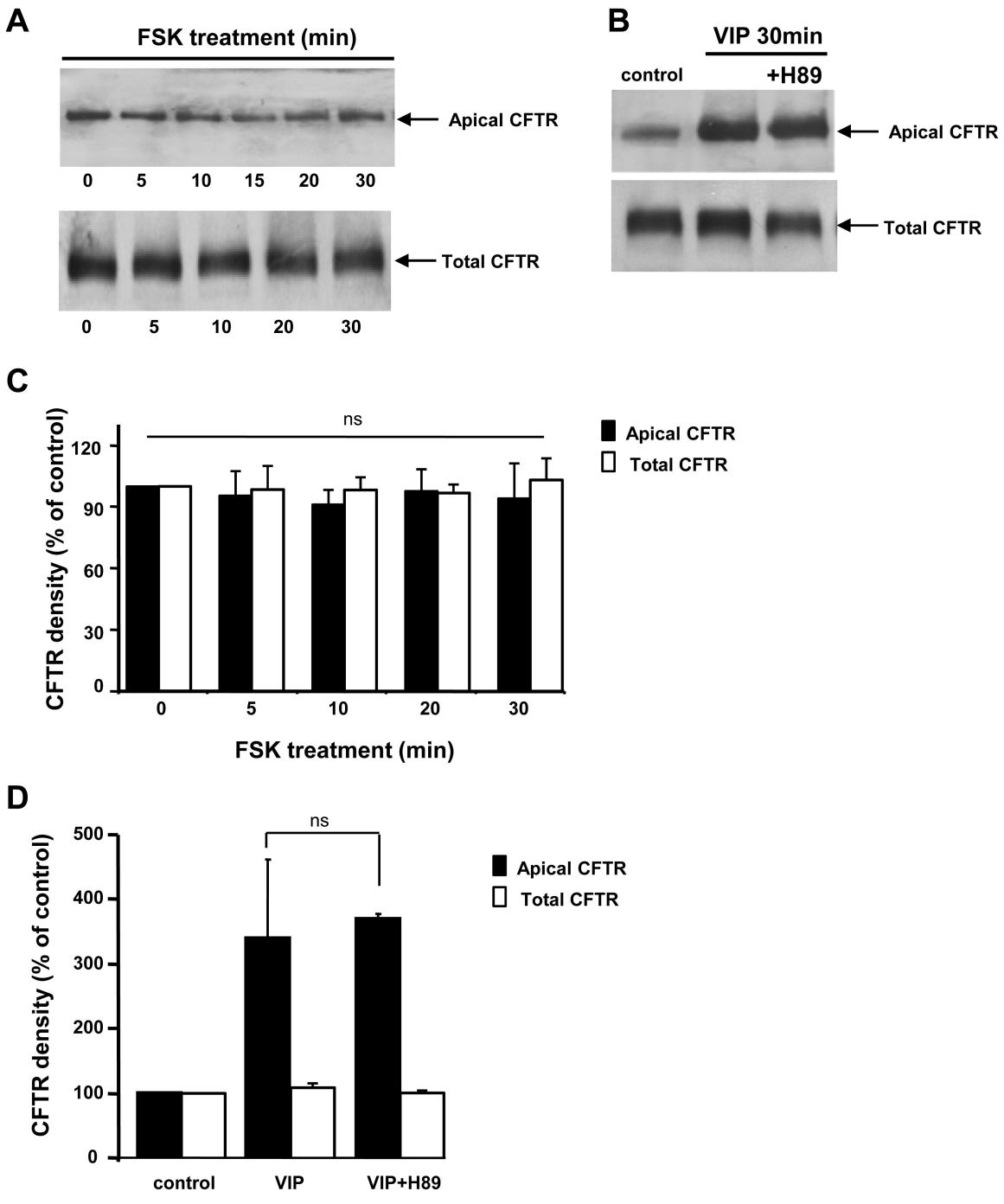
A
FSK treatment (min)
Apical CFTR
0 5 10 15 20 30
Total CFTR
0 5 10 20 30
B
VIP 30min
control
+H89
Apical CFTR
Total CFTR
C
ns
Apical CFTR
Total CFTR
CFTR density (% of control)
120
90
60
30
0
0 5 10 20 30
FSK treatment (min)
D
ns
Apical CFTR
Total CFTR
CFTR density (% of control)
500
400
300
200
100
0
control
VIP
VIP+H89

Figure 5

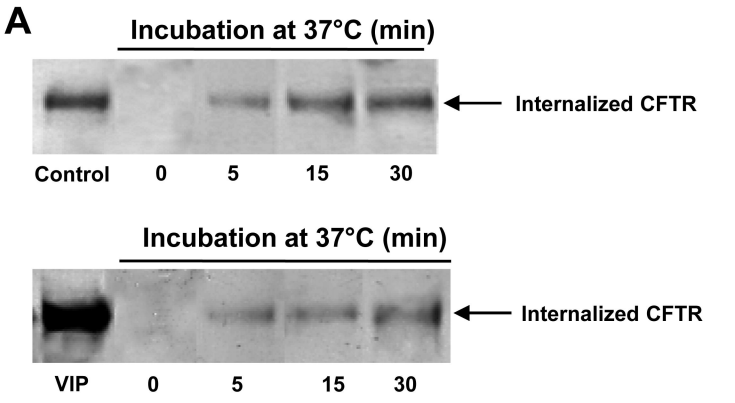
A
Incubation at 37°C (min)
Internalized CFTR
Control
0
5
15
30
Incubation at 37°C (min)
Internalized CFTR
VIP
0
5
15
30

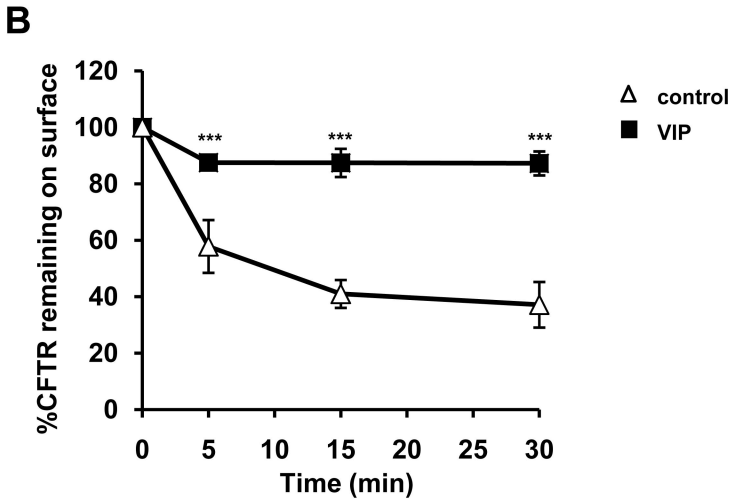
B
%CFTR remaining on surface
120
100
80
60
40
20
0
***
***
***
0
5
10
15
20
25
30
Time (min)
control
VIP

Figure 6

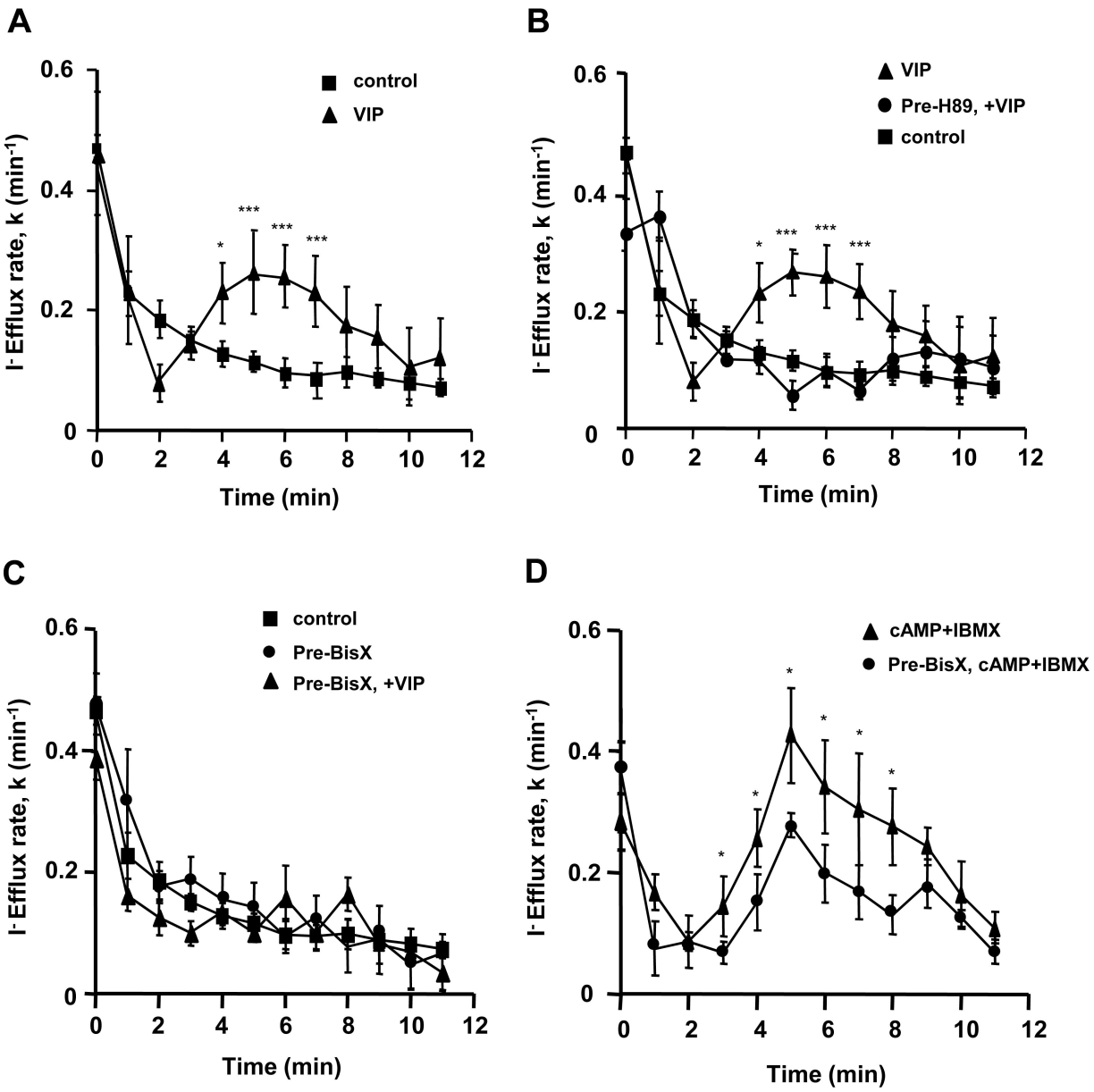
A
B
C
D
control
VIP
Pre-H89, +VIP
Pre-BisX
Pre-BisX, +VIP
cAMP+IBMX
Pre-BisX, cAMP+IBMX
I- Efflux rate, k (min-1)
Time (min)
0.6
0.4
0.2
0
0
2
4
6
8
10
12
*
***

Figure 7

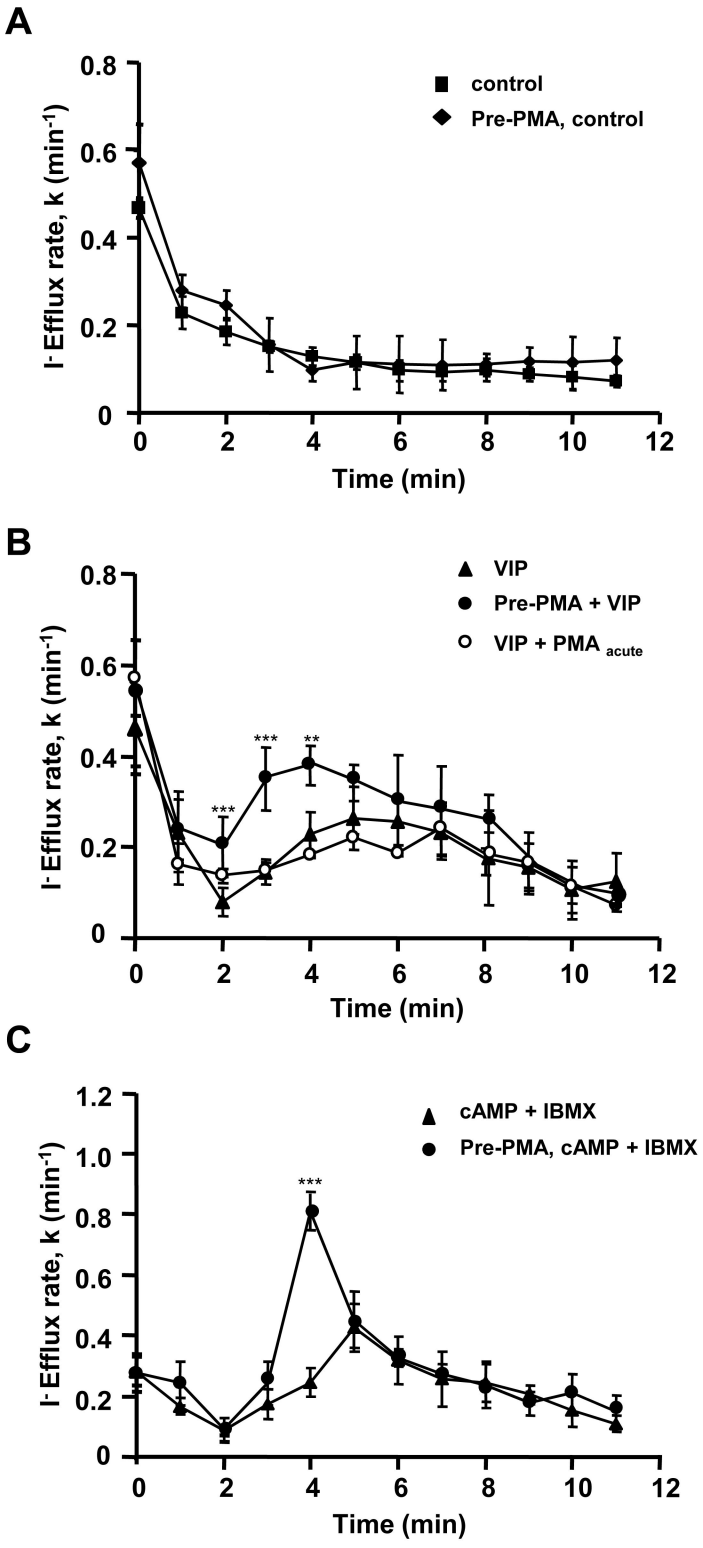
A
0.8
0.6
0.4
0.2
0
I⁻ Efflux rate, k (min⁻¹)
control
Pre-PMA, control
0
2
4
6
8
10
12
Time (min)
B
VIP
Pre-PMA + VIP
VIP + PMA acute
***
***
**
C
cAMP + IBMX
Pre-PMA, cAMP + IBMX
***
1.2
1.0

Figure 8

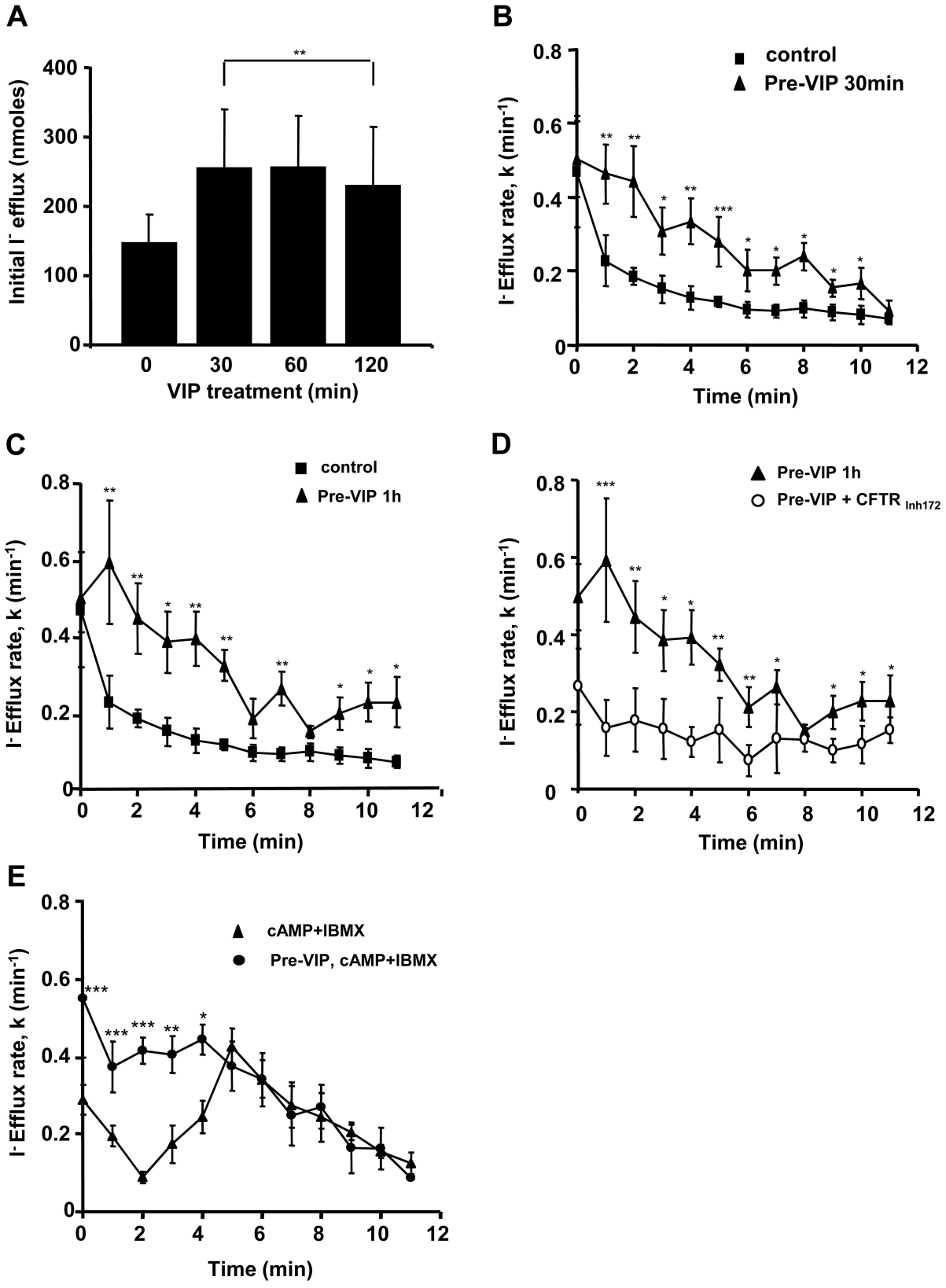
A
Initial I⁻ efflux (nmoles)
400
300
200
100
0
**
0
30
60
120
VIP treatment (min)
B
control
Pre-VIP 30min
I⁻ Efflux rate, k (min⁻¹)
0.8
0.6
0.4
0.2
0
0
2
4
6
8
10
12
Time (min)
C
control
Pre-VIP 1h
I⁻ Efflux rate, k (min⁻¹)
Time (min)
D
Pre-VIP 1h
Pre-VIP + CFTR Inh172
I⁻ Efflux rate, k (min⁻¹)
Time (min)
E
cAMP+IBMX
Pre-VIP, cAMP+IBMX
I⁻ Efflux rate, k (min⁻¹)
Time (min)

Figure 9

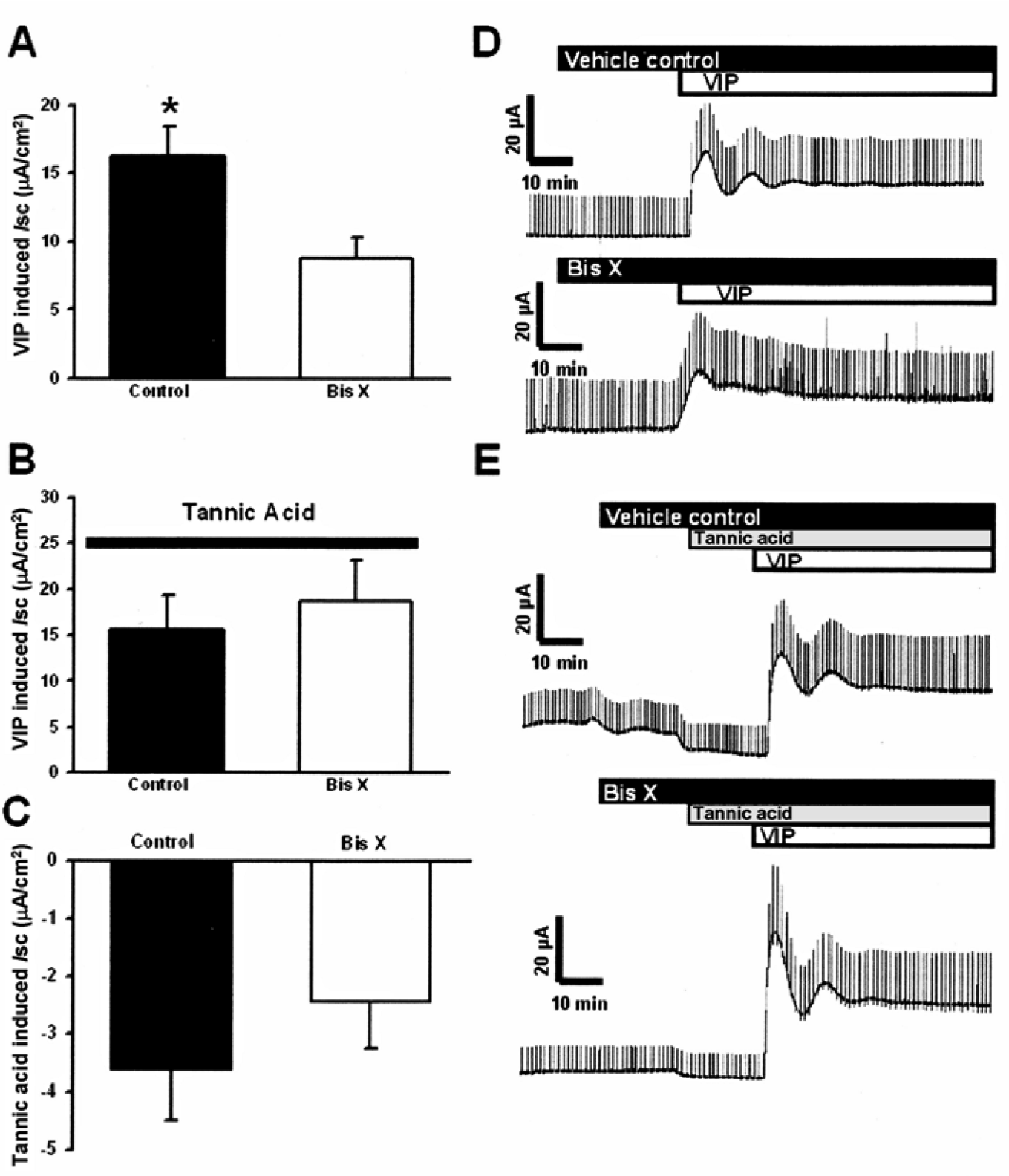
A
VIP induced Isc (μA/cm²)
20
15
10
5
0
*
Control
Bis X
B
Tannic Acid
VIP induced Isc (μA/cm²)
30
25
20
15
10
5
0
Control
Bis X
C
Control
Bis X
Tannic acid induced Isc (μA/cm²)
0
-1
-2
-3
-4
-5
D
Vehicle control
VIP
20 μA
10 min
Bis X
VIP
20 μA
10 min
E
Vehicle control
Tannic acid
VIP
20 μA
10 min
Bis X
Tannic acid
VIP
20 μA
10 min